Sensorless Control of Permanent Magnet Synchronous Motor Using Voltage Signal Injection

P. Brandstetter[1], T. Krecek[1]
[1]*Department of Electronics, VSB - Technical University of Ostrava,*
17. listopadu 15/2172, 708 33 Ostrava, Czech Republic
pavel.brandstetter@vsb.cz

***Abstract*—A successful application of vector control is subject to knowing the position of the rotor and, in synchronous machines, the knowledge of the initial position for a problem-free start-up. The ability to read rotor position and perform the vector control algorithm without a position sensor is typically referred to as sensorless vector control. Traditional feedback from the rotor position sensor, or the sensor of mechanical angular velocity of the motor, is typically replaced with a computational block or an algorithm that uses the measured voltage and current to indicate the actual position of the motor. The article presents a sensorless control of the permanent magnet synchronous motor using an injection of high frequency voltage for rotor position estimation.**

***Index Terms*—Vector control, sensorless control, voltage injection method, permanent magnet synchronous motor.**

I. INTRODUCTION

Permanent magnet synchronous motors are deployed in applications that are the most demanding in terms of dynamics. The disadvantage of the rather strenuous control of the position, torque, and speed which AC machinery had over DC machines was removed by the application of modern control methods which include vector control and direct torque control. Modern control systems with signal processors enabled realization of these methods [1]–[9].

The properties of a given Permanent Magnet Synchronous Motor (PMSM) depend, for the most part, on the position of the permanent magnets (PM) inside the motor. The PM may be installed in various ways. The basic methods are: a) Surface Mounted Permanent Magnet Synchronous Motor - SMPMSM, b) Interior Permanent Magnet Synchronous Motor - IPMSM) [10].

A successful application of vector control is subject to knowing the position of the rotor and, in synchronous machines, the knowledge of the initial position for a problem-free start-up. That is the reason why PMSM feature a position sensor that is fitted to the machine shaft. The ability to read rotor position and perform the vector control algorithm without a position sensor is typically referred to as sensorless vector control.

Most of the proposed methods of estimating the position of the rotor, or the mechanical angular velocity, are based on the measurement and processing of the basic parameters of the stator, i.e. stator current and voltage, to discover the amplitude and orientation of the magnetic flux in the machine. The methods are based on the mathematical model of the machine. Estimators and observers are used for the purpose of estimating the position of the rotor [11].

Methods based on the mathematical model of the machine are not suitable for applications that require the machine to operate at low speeds. This requirement has resulted in the development of methods that do not use the mathematical model of the machine, which rely on the so-called magnetic saliency, and is defined as the difference between transverse and longitudinal inductance.

The monitoring of magnetic saliency projected in the variation of stator inductance uses measurement of response to additional voltage or current signal, the frequency of which is higher than the frequency on the supply.

The study of magnetic saliency to estimate the position or velocity of the rotor by injection of signal with higher frequency has been the subject of global scientific research for several years. It is possible to use saturation magnetic saliency or other types of saliencies, e.g. spatial modulation of rotor leakage inductance caused by the grooves in the rotor. Some studies also estimate the position by the variance of rotor resistance or of leakage inductance.

Only two basic injection methods for getting information on the position of magnetic saliency (thus the position of the rotor) of PMSM are known to date. Injection methods are based on the measurement of stator current response while continuous high frequency voltage signal (High Frequency Injection Method) or sampling pulses (Transient Injection Method) are injected into the stator winding.

The method using sampling pulses injects measuring pulses into the voltage input channel. The injection signal is typically generated using a modified PWM method or by application of specific power-on states, upon which current response is measured. The process is performed at discrete times. It is vital that the onset of the measuring be exactly

Manuscript received April 21, 2012; accepted April 18, 2013.

The article has been elaborated in the framework of the IT4Innovations Centre of Excellence project, reg. no. CZ.1.05/1.1.00/02.0070 funded by Structural Funds of the European Union and state budget of the Czech Republic and in the framework of the project SP2013/118 which was supported by Student Grant Competition of VSB-TU of Ostrava.

synchronized with the injected measurement pulses. The most widely known method of this group is INFORM (INdirect Flux detection by On-line Reactance Measurement). The method is suitable for AC machines with geometric magnetic saliency such as the IPMSM [12], [13].

This paper looks into a method of assessing the position of a PMSM rotor with injection of continuous, high-frequency voltage signal.

II. List of the Used Symbols

$\mathbf{u}_{S\alpha\beta}$ stator voltage vector in [α, β] coordinate system;
$\mathbf{u}_{hf\alpha\beta}$ vector of the injected high frequency voltage in [α, β] coordinate system;
$\mathbf{i}_{S\alpha\beta}$ stator current vector in [α, β] coordinate system;
I_b base current for the current scaling;
$\boldsymbol{\psi}_{m\alpha\beta}$ rotor flux vector in [α, β] coordinate system;
Ψ_{PM} maximum value of magnetic flux created by PM;
R_S stator resistance;
$\mathbf{L}_{\alpha\beta}$ matrix of the stator inductances in [α, β] system;
L_S mean value of the stator inductance;
L_0 mean value of the magnetizing inductance;
L_σ leakage stator inductance;
ΔL_S amplitude of the stator inductance;
ΔL amplitude of the magnetizing inductance;
L_d, L_q stator inductances in [d, q] coordinate system;
L_δ, L_γ stator inductances in [δ, γ] coordinate system;
i_{Sd}, i_{Sq} stator current component in [d, q] system;
i_{S_ref} reference stator current;
ε rotor angle;
$\hat{\varepsilon}$ estimated rotor angle;
$\Delta\varepsilon$ angle shift of the magnetic saliency;
ε_m angle of the magnetic saliency;
$\hat{\varepsilon}_m$ estimated angle of the magnetic saliency;
ω_{hf} angular speed of the injected high frequency voltage;
ω_{sw} switching angular speed;
ω_{R_ref} reference rotor angular speed;
ω_R real rotor angular speed;
$\hat{\omega}_R$ estimated rotor angular speed.

III. Mathematical Model of the PMSM

We can derive a mathematical model of the IPMSM in the stator coordinates [α, β]:

$$\mathbf{u}_{S\alpha\beta} = R_S \mathbf{i}_{S\alpha\beta} + \frac{d}{dt}\left[\mathbf{L}_{\alpha\beta}\,\mathbf{i}_{S\alpha\beta} + \boldsymbol{\psi}_{m\alpha\beta}\right], \tag{1}$$

$$\mathbf{L}_{\alpha\beta} = \begin{bmatrix} L_S - \Delta L_S\cos(2\varepsilon) & -\Delta L_S\sin(2\varepsilon) \\ -\Delta L_S\sin(2\varepsilon) & L_S + \Delta L_S\cos(2\varepsilon) \end{bmatrix}, \tag{2}$$

$$L_S = L_\sigma + \tfrac{3}{2}L_0, \Delta L_S = \tfrac{3}{2}\Delta L, \tag{3}$$

$$\boldsymbol{\psi}_{m\alpha\beta} = \Psi_{PM}\begin{bmatrix}\cos(\varepsilon)\\ \sin(\varepsilon)\end{bmatrix}. \tag{4}$$

IV. Magnetic Saliency of the PMSM

A necessary requirement of the injection method is a known magnetic saliency ($L_d \neq L_q$) in the machine so that a position or flux dependent inductance results.

There are several sources of saliencies in PM machines. For example: rotor inherent saliency, saturation base saliency (yoke, teeth), rotor stator teeth harmonics, lamination direction based saliency, eddy current based saliency, rotor eccentricity saliency etc. [14].

Saliency of the PMSM is mainly caused by two dominant effects: geometrical construction of rotor (rotor inherent saliency) such as the IPMSM, and magnetic saturation of the stator, which appears in all type of the PMSMs. The IPMSMs exhibit the most saliency (L_q = 2 to 3 times L_d) and the SMPMSMs exhibit a very small saliency ($L_d \approx L_q$). In this paper a single saliency is consideration: rotor construction (rotor inherent) saliency and saturation induced saliency.

A number of factors exist that might change under various machine loads and which result in a shift of the resulting magnetic flux. They are primarily: (a) magnetic flux, (b) saturation level, (c) flux orientation, (d) orientation of saturation and (e) change of saturation areas [14].

For the sake of simplicity of the control strategy (injection methods address the low speed band), consider: $i_{Sd} = 0$ and $i_{Sq} = i_{S\_ref}$. Therefore, to shift the resulting magnetic flux, the following applies

$$\Delta\varepsilon \approx \arcsin\left(\frac{i_{Sq}L_q}{\sqrt{{\Psi_{PM}}^2 + \left(i_{Sq}L_q\right)^2}}\right) \tag{5}$$

Spatial shift of the resulting magnetic flux is modeled by shifting the basic saliency by the angle $\Delta\varepsilon$.

In (1) is then used the modified equation (2) using angle of the magnetic saliency ε_m:

$$\mathbf{L}_{\alpha\beta(\Delta\varepsilon)} = \begin{bmatrix} L_S - \Delta L_S\cos(2\varepsilon_m) & -\Delta L_S\sin(2\varepsilon_m) \\ -\Delta L_S\sin(2\varepsilon_m) & L_S + \Delta L_S\cos(2\varepsilon_m) \end{bmatrix}, \tag{6}$$

$$L_S = \left(L_\delta + L_\gamma\right)/2, \Delta L_S = \left(L_\gamma - L_\delta\right)/2, \tag{7}$$

$$\varepsilon_m = \varepsilon + \Delta\varepsilon. \tag{8}$$

V. Voltage Injection Methods

There are several methods of voltage signal injection: injection of the rotating signal in coordinates [α, β], injection of the rotating signal in coordinates [d, q] and injection of the pulsating signal in coordinates [d, q] [15].

For the voltage signal injection in the coordinate system [α, β], voltage vector $\mathbf{u}_{hf\alpha\beta}$ with amplitude U_{hf} is used that rotates with angular frequency ω_{hf}

$$\mathbf{u}_{hf\alpha\beta} = U_{hf}\begin{bmatrix}-\sin\left(\omega_{hf}t\right)\\ \cos\left(\omega_{hf}t\right)\end{bmatrix}, \tag{9}$$

The frequency of injected voltage signal is within the range 500 Hz -1 kHz. At this frequency, $\omega_{hf}L_s >> R_s$ and (1) with respect to (6) can be simplified

$$\begin{bmatrix}u_{Shf\alpha}\\ u_{Shf\beta}\end{bmatrix} = \frac{d}{dt}\left\{\mathbf{L}_{\alpha\beta(\Delta\varepsilon)}\begin{bmatrix}i_{Shf\alpha}\\ i_{Shf\beta}\end{bmatrix}\right\}. \tag{10}$$

By substituting (9) to (10), we obtain after adjustment:

$$\begin{bmatrix} i_{Shf\,\alpha} \\ s_{Shf\,\beta} \end{bmatrix} = K_I \begin{bmatrix} L_S \cos\left(\omega_{hf} t\right) + \Delta L_S \cos\left(2\varepsilon_m - \omega_{hf} t\right) \\ L_S \sin\left(\omega_{hf} t\right) + \Delta L_S \sin\left(2\varepsilon_m - \omega_{hf} t\right) \end{bmatrix}, \quad (11)$$

$$K_I = \frac{U_{hf}}{\omega_{hf} L_\delta L_\gamma} \quad (12)$$

The resulting current consists of two components. The first component is proportional to the mean value of the stator inductance. This component does not contain information about the rotor position and therefore becomes a parasitic. The second component is directly proportional to the difference of the stator inductances ΔL_S that can be understood as magnetic saliency. This component contains useful information about the rotor position, respectively magnetic saliency.

The current of higher frequency can be obtained from the basic frequency by band-pass filter. Position information can be derived from (11)

$$\mathbf{i}_{\mathrm{Shf}\alpha\beta} = \mathbf{i}_{\mathrm{Shf\_p}} + \mathbf{i}_{\mathrm{Shf\_n}} = K_I \begin{bmatrix} L_S e^{j\omega_{hf} t} + \\ + \Delta L_S e^{j\left(2\hat{\varepsilon}_m - \omega_{hf} t\right)} \end{bmatrix}, \quad (13)$$

where $\mathbf{i}_{\mathrm{Shf\_p}}$ is positively rotating current component and $\mathbf{i}_{\mathrm{Shf\_n}}$ is negatively rotating current component.

To extract the position information we can use the principle of mixing or so-called synchronous filter. The resulting block implementation is shown in Fig. 1.

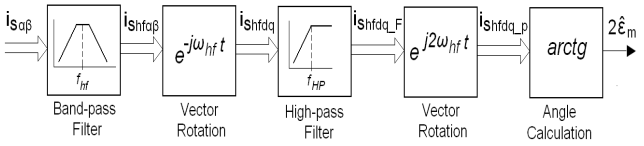

Fig. 1. Synchronous filter for demodulation of HF current vector.

The signal corresponding to the current in [α, β] coordinates enters in the block of the band-pass filter. In this block, the signal with higher frequency is separated from the signal with fundamental frequency. The current component with the higher frequency enters in the block Synchronous Filter where the demodulation is realized in the following steps.

Coordinate transformation into a system identical to the injected signal

$$\begin{bmatrix} i_{Shfd} \\ i_{Shfq} \end{bmatrix} = K_I \begin{bmatrix} L_S + \Delta L_S \cos\left(2\hat{\varepsilon}_m - 2\omega_{hf} t\right) \\ L_S + \Delta L_S \sin\left(2\hat{\varepsilon}_m - 2\omega_{hf} t\right) \end{bmatrix}. \quad (14)$$

Filtration of DC component

$$\begin{bmatrix} i_{Shfd\_F} \\ i_{Shfq\_F} \end{bmatrix} = FHP\left(\begin{bmatrix} i_{Shfd} \\ i_{Shfq} \end{bmatrix}\right) = K_I \begin{bmatrix} \Delta L_S \cos\left(2\hat{\varepsilon}_m - 2\omega_{hf} t\right) \\ \Delta L_S \sin\left(2\hat{\varepsilon}_m - 2\omega_{hf} t\right) \end{bmatrix}. \quad (15)$$

Transformation to the rotating system with double angular speed of the injected signal

$$\begin{bmatrix} i_{Shfd\_p} \\ i_{Shfq\_p} \end{bmatrix} = \begin{bmatrix} i_{Shfd\_F} \\ i_{Shfq\_F} \end{bmatrix} e^{j2\omega_{hf} t} = K_I \begin{bmatrix} \Delta L_S \cos\left(2\hat{\varepsilon}_m\right) \\ \Delta L_S \sin\left(2\hat{\varepsilon}_m\right) \end{bmatrix}. \quad (16)$$

Estimated angle of the magnetic saliency can be obtained as follows

$$\hat{\varepsilon}_m = \frac{1}{2} arctg\left(\frac{i_{Shfq\_p}}{i_{Shfd\_p}}\right). \quad (17)$$

VI. Parameter Selection for the Injection Method

The injection methods require for obtaining a quality signal of the position and speed estimation appropriately to choose the amplitude and frequency of the injected signal, as well as the appropriate frequency band width of all used filters, current, speed and position controllers.

The maximum frequency of the injected signal can be chosen as follows [16]

$$10\omega_{hf} \le \omega_{sw}. \quad (18)$$

The amplitude of the injected voltage can be approximately estimated from the following equation [16]

$$U_{hf} \ge \frac{I_b \omega_{hf} L_\delta L_\gamma}{10\Delta L_S}. \quad (19)$$

VII. Experimental Laboratory Workplace

The laboratory system consists of an electrical drive, control system of the drive, and a superimposed and a measuring station. The realized laboratory model is shown in Fig. 2.

The mechanical part of the drive contains a permanent magnet synchronous motor and a loading asynchronous motor.

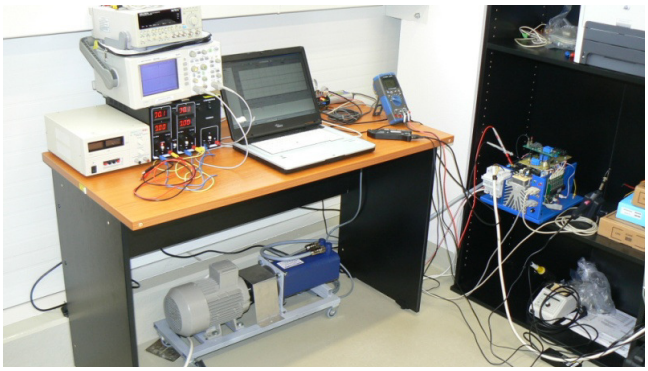

Fig. 2. Experimental laboratory stand.

The controlling element is a Freescale DSP 56F8037 digital signal processor. The base board with the DSP also contains a transducer of the serial line to USB; therefore, communication and data acquisition uses the USB interface.

The program is loaded and tuned via the USB interface with a USB TAP by Freescale.

The base board uses general purpose input and output of the DSP (GPIO) to receive measurement signals and emits control signals via the expansion board. The expansion board modifies, amplifies and changes partial signals so that the processor can evaluate them [17].

The main parameters of the IPMSM used are shown in Table I. The IPMSM used features an incremental sensor that uses 2048 pulses per revolution.

TABLE I. PARAMETERS OF THE USED IPMSM.

Nominal torque	7.7 Nm
Nominal current	5.65 A
Maximal demagnetizing current	26 A
Nominal speed	3000 rpm
Number of magnetic pole pairs	2
Nominal power	2.42 kW
Voltage constant	0.7 V/rad
Longitudinal inductance	1.75 mH
Transverse inductance	4.9 mH
Stator resistance	1.11 Ω
Moment of inertia	17.41 kgcm^2

VIII. EXPERIMENTAL RESULTS

As the sensorless PMSM drive with injection methods and with vector-oriented control is rather a complex system, it is suitable that the entire system be verified in a computer simulation after theoretical preparation and before the realization. The simulation results shown below were prepared in MATLAB /SIMULINK software.

The control structure from Fig. 3 was used for the simulation of injection methods. Injected voltage was chosen at U_{hf} = 30 V and frequency f_{hf} = 1 kHz [17].

Fig. 4 shows the result of simulation of sensorless control with injection in coordinates [α, β]. Information on rotor position for the vector angle of the parameters and feedback is collected from the synchronous filter demodulator (Fig. 1).

The time courses of the variables in Fig. 4 represent the behaviour of the AC drive in the dynamic state. Stable behaviour of the drive is observed. The waving of rotor speed can be almost eliminated by broadening the band of the speed loop; however, this comes at the expense of inferior drive dynamics.

Properties in control to zero speed (therefore the properties of the sensorless drive at zero speed) are shown in Fig. 5. Speed is controlled to a zero value until (and when) load torque occurs. Evidence suggests that the drive is stable and accurate also at zero speed.

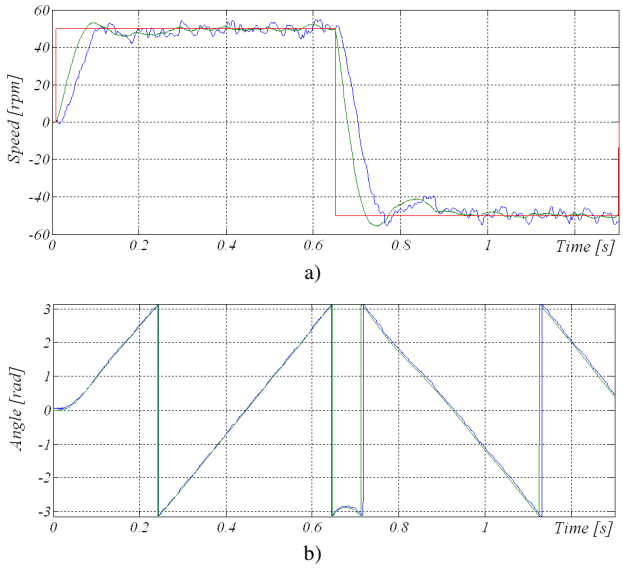

Fig. 4. Response of the basic variables, change of the reference speed 0 → 50 rpm and reversation to – 50 rpm without the load, reference speed (red), real speed (green), estimated speed (blue), real rotor angle (blue), estimated rotor angle (green).

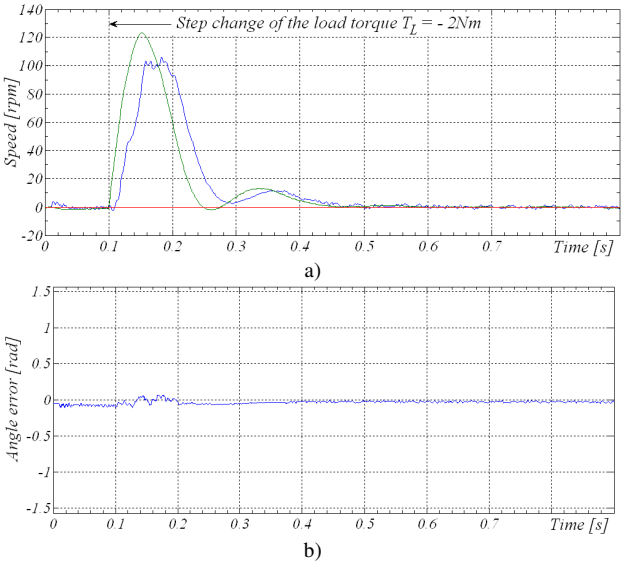

Fig. 5. Response of the basic variables, control at zero speed and drive behavior at step change of the load torque, real speed (green), estimated speed (blue).

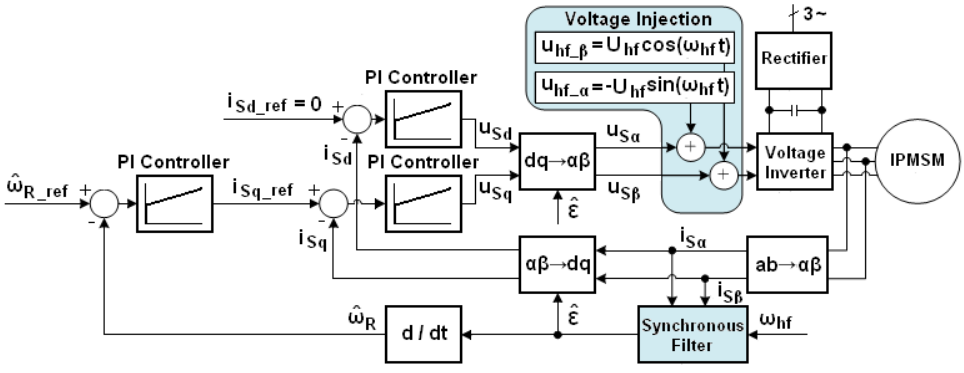

Fig. 3. Control structure of the AC drive with the PMSM.

One of the principal limitations of the injection methods is the deformation of the useful component of current response by distortion of the injected voltage from the non-linearity of the voltage inverter, especially the dead-time. This non-linearity is produced by additional components in the resulting current response which invalidate the position information in the signal.

The output from the position estimator (see Fig. 1) is not the actual position of the rotor but the position of the magnetic saliency. When load occurs, the saturated areas are changed by stator currents and a phase shift occurs in the actual position and in the position of magnetic saliency.

If the position of the saliency is the output, the indicated position requires corrections. The angle of saturation may be obtained by measurement or, when a lower degree of accuracy is assumed, a formula may be used for such purpose

$$\Delta\varepsilon \approx \text{arctg}\left(\frac{i_{Sq}L_q}{\Psi_{PM}}\right)+\varphi\,, \tag{20}$$

where φ is phase shift caused by the current controller and hardware filter. The principle of compensation is shown in Fig. 6.

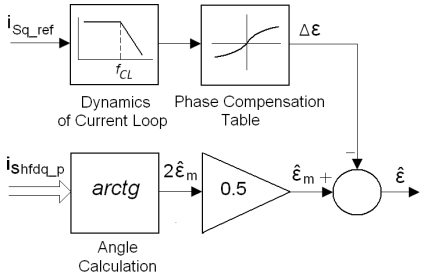

Fig. 6. Principle of angle shift correction.

As the position of the magnetic saliency is affected by the magnetic flux of the stator, the phase shift dynamics can be emulated by the dynamics of the current loop. A low-pass filter and the required value of current represent this emulation in the structure.

The resulting current is used for addressing the phase compensation table. The resulting angle of saturation is subtracted from the actual position of the magnetic saliency to obtain the true position of the rotor; the position may also be used for addressing the SMP table.

An experimental compensation test is shown in Fig. 7. The compensation table contained 16 values and they were selected using linear approximation. The table elements were calculated using (20).

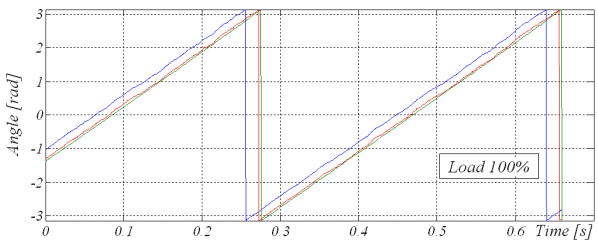

Fig. 7. Compensation of the angle shift, real rotor angle (green), estimated rotor angle (red), estimated angle of magnetic saliency (blue).

The figures below present experimental verification of the injection method in coordinates [α, β]. Injection uses hardware compensation of the dead time in the inverter; this improves the quality of position signals ergo the properties of sensorless control [17].

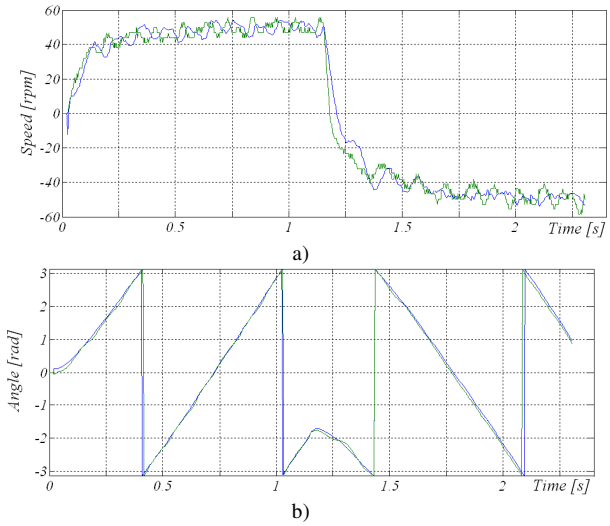

Fig. 8. Response of the basic variables, change of the reference speed 0 → 50 rpm and reversation to – 50 rpm with the load, real speed (green), estimated speed (blue), real rotor angle (blue), estimated rotor angle (green).

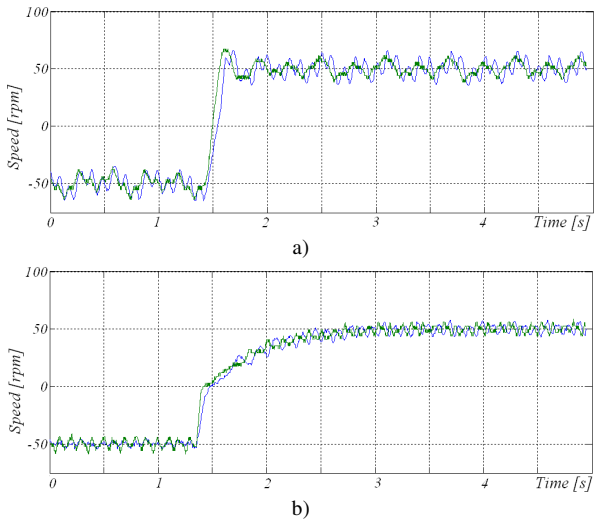

Fig. 9. Speed responses, change of the reference speed +50 rpm → – 50 rpm without the load and with the load (50%), real speed (green), estimated speed (blue).

Fig. 8 shows the behaviour of a sensorless drive at startup and reverse change of direction under load. The drive goes through dynamic states without showing symptoms of instability. However, increased position errors in the dynamic states are worth mentioning.

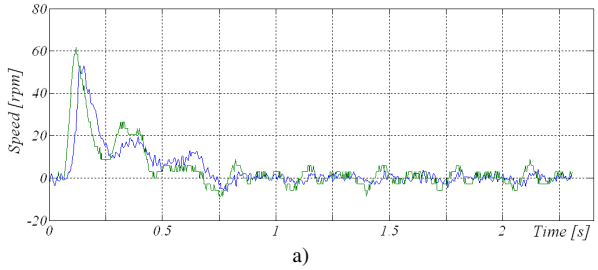

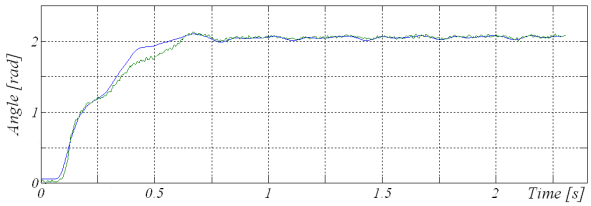

b)

Fig. 10. Response of the basic variables, control at zero speed and drive behavior at step change of the load torque, real speed (green), estimated speed (blue), real rotor angle (blue), estimated rotor angle (green).

The phenomenon is caused by transition events that occur inside the current loop circuit.

Sensorless drive was tested at reverse change of direction from -50 rpm to +50 rpm. The result of the drive behaviour under this dynamic state is shown in Fig. 9.

In the last measuring session, the sensorless drive was tested for response at abrupt changes of torque load at zero speeds. The results of the measurement are shown in Fig. 10. The drive system has stable performance at any levels of load.

IX. CONCLUSIONS

In methods based on the machine model, drive utilization at zero and low speeds is highly problematic and complicated. Therefore, injection methods have been developed that are capable of curbing the issues of the low speed band in the sensorless drive provided the machine is magnetically asymmetrical. Besides the basic harmonic power supply voltage, the output inverter must generate additional voltage with higher frequency; therefore, additional losses are generated in the machine per se and in the output inverter. The fact is naturally one of the disadvantages of the injection methods. As the high frequency voltage is superimposed to the basic harmonic of the supply voltage, the available value of the basic harmonic is reduced by the injection; if voltage is injected across the entire range of speed, the maximum available value of drive speed is reduced as well. However, injection methods are typically used in the lower speed band.

The results of the simulation and experiments have validated the theory of injection method and have proven them to be suitable for both low- and zero speeds.

REFERENCES

[1] P. Vas, *Sensorless Vector and Direct Torque Control*. Oxford University Press, 1998.

[2] P. Chlebis, P. Moravcik, P. Simonik, "New Method of Direct Torque Control for Three–Level Voltage Inverter", in *Proc. of the EPE Conf.*, Barcelona, 2009, pp. 4051–4056.

[3] D. Uzel, Z. Peroutka, "Optimal Control and Identification of Model Parameters of Traction Interior Permanent Magnet Synchronous Motor Drive", in *Proc. of IECON*, Melbourne, 2011, pp. 1960–1965.

[4] L. Qin, X. C. Zhou, P. J. Cao, "New Control Strategy for PMSM Driven Bucket Wheel Reclaimers using GA–RBF Neural Network and Sliding Mode Control", *Elektronika ir Elektrotechnika (Electronics and Electrical Engineering*), no. 6, pp. 113–116, 2012.

[5] A. Cifci, Y. Uyaroglu, S. Birbas, "Direct Field Oriented Controller Applied to Observe Its Advantages over Scalar Control", *Elektronika ir Elektrotechnika (Electronics and Electrical Engineering*), no. 9, pp. 15–18, 2012.

[6] J. Vittek, P. Bris, P. Makys, M. Stulrajter, "Forced Dynamics Control of PMSM Drives with Torsion Oscillations", *Journal COMPEL*, vol. 29, no. 1, pp. 187–204, 2010. [Online]. Available: http://dx.doi.org/10.1108/03321641011008046

[7] D. Perdukova, P. Fedor, "Simple Method of Fuzzy Linearization of Non–Linear Dynamic System", *Acta Technica CSAV*, vol. 55, no. 1, pp. 97–111, 2010.

[8] P. Spanik, P. Drgona, M. Frivaldsky, A. Prikopova, "Design and Application of Full Digital Control System for LLC Multiresonant Converter", *Elektronika ir Elektrotechnika (Electronics and Electrical Engineering*), no. 10, pp. 75–78, 2010.

[9] A. Daubaras, M. Zilys, "Vehicle Detection based on Magneto–Resistive Magnetic Field Sensor", *Elektronika ir Elektrotechnika (Electronics and Electrical Engineering*), no. 2, pp. 27–32, 2012.

[10] F. J. Gieras, M. Wing, *Permanent Magnet Motor Technology: Design and Applications*. CRC Press, 2002.

[11] L. Jones, J. Lang, "A State Observer for the Permanent–Magnet Synchronous Motor", *IEEE Transactions on Industrial Electronics*, vol. 36, pp. 374–382, 1989. http://dx.doi.org/10.1109/41.31500

[12] M. Schroedl, "Sensorless Control of AC Machines at Low Speed and Standstill Based on the "INFORM" Method", in *31st Conference Record of IEEE Industry Applications Conference*, 1996, vol. 1, pp. 270–277.

[13] P. L. Jansen, R. D. Lorenz, "Transducerless Position and Velocity Estimation in Induction and Salient AC Machines", *IEEE Transactions on Industry Applications*, vol. 31, pp. 240–247, 1995. http://dx.doi.org/10.1109/28.370269

[14] S. Overbo, R. Nilssen, "High Frequency Flux Distribution in Permanent Magnet Synchronous Machines", in *Proc. of NORPIE Conf.*, Trondheim, 2004.

[15] M. Linke, R. Kennel, J. Holtz, "Sensorless Speed And Position Control of Synchronous Machines Using Alternating Carrier Injection", in *Proc. IEEE International Conference Electric Machines and Drives*, 2003, vol. 2, pp. 1211–1217.

[16] O. Wallmark, "Control of Permanent–Magnet Synchronous Machines in Automotive Applications", Ph.D. dissertation, Chalmers University of Technology, Sweden, 2006.

[17] T. Krecek, "Sensorless Control of Permanent Magnet Synchronous Motor in the Area of Low Speed", Ph.D. dissertation, VSB – Technical University of Ostrava, 2009.